Back analysis of a building collapse under snow-and-rain loads in Mediterranean area

Isabelle Ousset[1], Guillaume Evin[1], Damien Raynaud[1], and Thierry Faug[1]

[1]Univ. Grenoble Alpes, CNRS, INRAE, IRD, Grenoble INP*, IGE, 38000 Grenoble, France. *Institute of Engineering and Management Univ. Grenoble Alpes.

Correspondence: Isabelle Ousset (isabelle.ousset@inrae.fr)

Abstract. At the end of February 2018 the Mediterranean area of Montpellier in France was struck by a significant snowfall that turned into an intense rain event caused by an exceptional atmospheric situation. This rain-on-snow event produced pronounced damage to many buildings of different types. In this study, we report a detailed back analysis of the roof collapse of a large building, namely the Irstea Cévennes building. Attention is paid to the dynamics of the climatic event, on the one hand, and to the mechanical response of the metal roof structure to different snow-and-rain loads, on the other hand. The former aspect relies on multiple sources of information that provide reliable estimates of snow heights in the area before the rain came into play and substantially modified the load on the roof. The latter aspect relies on detailed finite element simulations of the mechanical behavior of the roof structure in order to assess the pressure due to snow-and-rain loading which could theoretically lead to failure. By combining the two approaches, it is possible to reconstruct the most probable scenario for the roof failure before its full collapse. As an example of building behavior and vulnerability to an atypical rain-on-snow event in the Mediterranean area of France, this detailed case study provides useful key points to be considered in the future for a better mitigation of such events in non-mountainous areas.

1 Introduction

In the framework of snowfalls, there are a number of reported cases of roof collapses caused by snow loads outside mountainous areas. The following events that occurred during the two past decades can be mentioned:

- In France: the collapse of the roof of a warehouse at Satolas-et-Bonce in the Isère department and of a supermarket store at Bricquebec in the Manche department (January 2010), several collapses of roofs in Western France (at least nine store roofs in the Manche department) in March 2013, several damage to shops in the department of Hérault at the end of February 2018 in the cities of Béziers, Lattes, Montpellier, Peyrols (see examples shown in Figure 1).

- In Europe: the collapse of a self-weighted metallic roof in Spain in March 2004 (del Coz Díaz et al., 2012), the collapse of a public fair pavilion in Italy during February 2001 (Brencich, 2010), total collapse of the Katowice fair building in Poland which caused 65 deaths and 180 injuries in January 2006 (Biegus and Rykaluk, 2009), the collapse of the Bad Reichenhall Ice Rink roof in Germany which led to 15 deaths the same month (Winter and Kreuzinger, 2008), the

collapse of a gymnasium roof in Switzerland in 2009 (Piskoty et al., 2013), the collapse of a store hall in Gdansk (Poland) in February 2010 (Biegus and Kowal, 2013), collapse of a shopping facility in Poland during January 2015 (Krentowski et al., 2019).

- In other regions of the world: collapse of truss roof structures in Turkey in February 2003 (Caglayan and Yuksel, 2008) as well as during January and October 2015 (Piroglu and Ozakgul, 2016; Altunişik et al., 2017), many roof collapses in Northeastern United States (O'Rourke and Wikoff, 2014) during the winter 2010-2011.

The principal source of explanation given in the literature for these building collapses is a stronger (greater than the standard) snowfall hazard (Strasser, 2008; Holický and Sýkora, 2009; Geis et al., 2012; Le Roux et al., 2020). It should be noted that a poor design or insufficient material strengths may sometimes be identified as another main reason for the collapse (Biegus and Rykaluk, 2009; Caglayan and Yuksel, 2008; Brencich, 2010; del Coz Díaz et al., 2012; Biegus and Kowal, 2013; Piskoty et al., 2013; O'Rourke and Wikoff, 2014; Altunişik et al., 2017; Krentowski et al., 2019). In a large meta-analysis of building failures related to snow loads, Geis (2011) found that these incidents are commonly attributed to the large amount of snow, followed by problems in the design of the building, melting snow and rain-on-snow events.

Roof collapses due to rain-on-snow surcharges can happen in situations where the temperature is close to 0°C during the snow event. In the United States, the potential rain-on-snow surcharge of roof snow loads has been discussed in detail by O'Rourke and Downey (2001) and is taken into account in the building standards (ASCE, 2013). Canada considers the direct sum of the snow load and the rain load (Canadian Commission on Building and Fire Codes, 2010). Rain-on-snow surcharges have been the subject of several studies in Japan (Otsuki et al., 2016; Takahashi et al., 2016) following a rain-on-snow event that occurred in February 2014 in the Kanto region and where the additional rain on the snow load caused the collapse of many large span structures. Using controlled outdoor experiments where rain is added to a snow cover, Otsuki et al. (2017) show that rain contributes to a larger increase of the snow load for larger roofs with smaller slope angles, due to the time it takes for the water to reach the eaves. In Europe, Eurocode 1 provides the guidelines for the calculation of the design snow load (AFNOR, 2007). Eurocode 1 specifies that in areas where rain-on-snow may cause melting followed by frost, the values of loads due to snow on the roof must be increased, especially if snow and ice can block the roof drainage system. The NF EN 1991-1-3 standard stipulates that roof snow load must be increased by 0.2 kN.m^{-2} when the slope for water flow is lower than 3 %, in order to account for the snow density increase resulting from difficulties of water drainage in case of rain.

The current paper reports a detailed and specific case study of a roof collapse of a scientific laboratory (ex-Irstea, INRAE) which occurred on the 1st of March around 18:00 following an intense rain-on-snow event in a Mediterranean area. Several roof collapses took place in this area in the same period (see Figure 1).

Figure 2 shows the main damage observed during a field visit on 18 March 2018, shortly after the collapse of the experimental hall of the Irstea Cévennes building in the central part of the structure, in the east-west direction. The western and eastern facades were heavily damaged, as seen in Fig. 2a and 2c. On the contrary, the other two facades (see Figure 2b and 2d) were much less damaged due to the presence of the inner concrete walls of the offices and of the inner metal frames of the laboratory rooms along the southern and northern facades, respectively. Local damage observed on structural elements consists of (i)

Figure 1. Roof collapses due to heavy snowfalls occurred on 28 February and 1st March 2018 in the surroundings of Montpellier, France: collapses of (a) the shopping center Estanove in Montpellier (Photo credit: ©Jean-Michel Mart), (b) a car wash station in Lattes (Photo credit: ©Le Petit Journal de Lattes), (c) the Darty store in Peyrols (Photo credit: ©France 3 LR / S. Banus) and (d) a restaurant in La Grande Motte (Photo credit: ©France 3).

buckling and bending for the roof tubular profiles, (ii) bending and shear for the tubular supporting pylons and (iii) cracking on the walls of the offices (see close-up views of the damage shown in Figure S3 in the Supplementary Material (SM)).

60   This study aims at fulfilling the two following objectives: 1) What is the most likely load at the time of the collapse and how does it compare to the characteristic values (e.g. Eurocode Snow loads)? 2) What is the most likely scenario for the roof failure, i.e. how did the structure reach a critical state which led to its collapse? We first present the meteorological event consisting of a snowfall followed by rain at the time of the roof collapse in Section 2 using multiple sources of information: outputs from the AROME numerical model, which is the French fine-mesh numerical weather forecast service model, social network

65   testimonies and weather observations. Section 3 presents finite element simulations of the mechanical behavior of the building subject to different pressure fields representing snow-and-rain loads. Section 4 makes the link between Sections 3 and 2 and presents a detailed description of the most probable scenario for the roof collapse of Irstea Cévennes building. This example of a roof collapse caused by an intense rain-on-snow event that occurred in the Mediterranean area is also used to emphasize a number of questions that need to be addressed in the future, in particular, what improvements can be proposed to minimize the

70   risk of a roof collapse due to snow-and-rain loading in those areas.
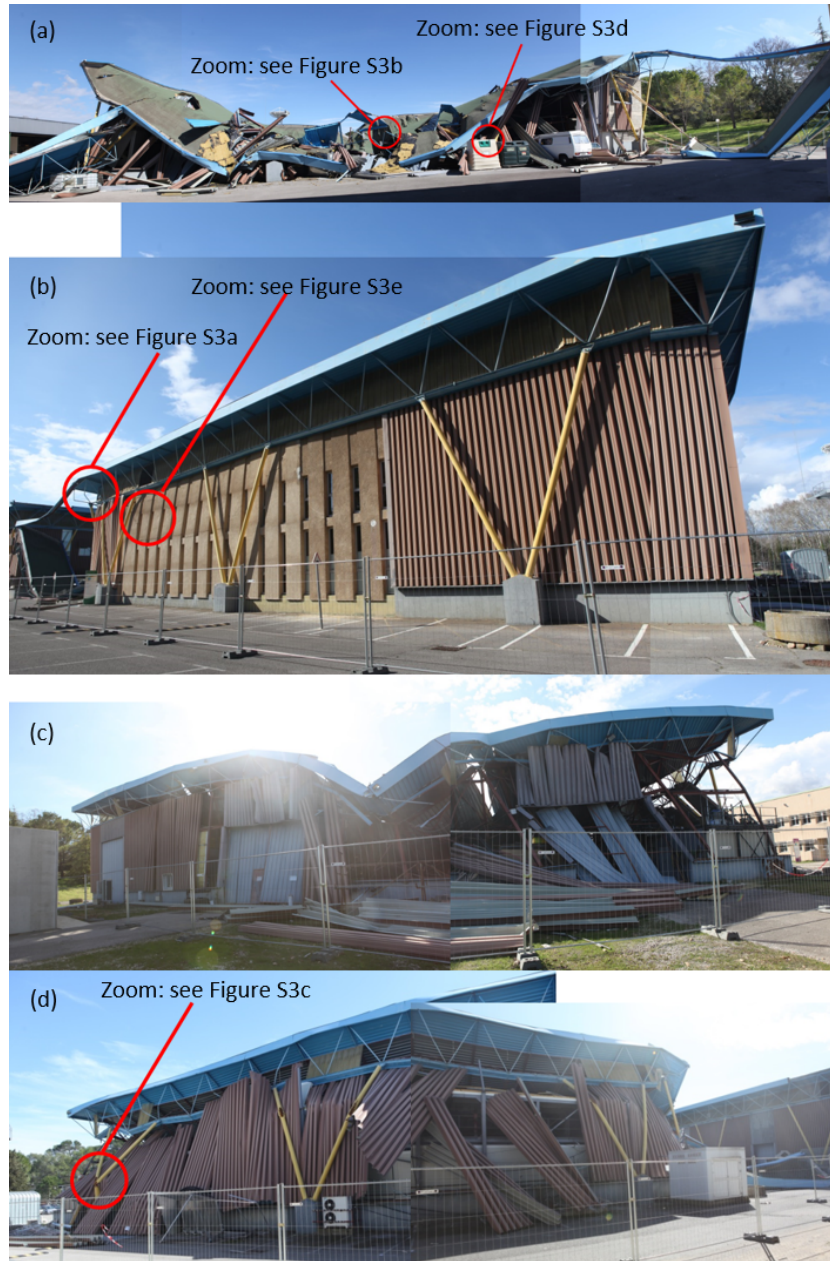
Figure 2. Different pictures showing the hierarchy of damage as observed on 18 March 2018 on the western (a), southern (b), eastern (c), and northern (d) facades of the Irstea Cévennes building.

2 Description of the meteorological event

2.1 An exceptional atmospheric situation

At the end of February 2018, France, and more generally Europe, was subject to wintry weather conditions. A disordered polar vortex unleashed a very cold air mass through central Europe around 24-25 Feb. Driven by a powerful anticyclone localized in Scandinavia and a sustained eastern flux, this cold spell spread over western Europe during the following days, resulting in the most intense cold spell over Europe since Feb. 2012 which is referred to as "Beast from the East".

Figure 3 presents the outputs of the high-resolution AROME model for different times and lead times. The regional AROME model assimilates various types of observations (radar, ground measurement data, radio, satellite radiances (see Bouttier and Roulet (2008)) and must be interpreted with care. AROME outputs provide interesting information regarding the spatio-temporal dynamics of the meteorological event. Four parameters are represented: temperature at 850 hPa, temperature at 2 m, wind at 10 m, and precipitation amount accumulated in 1 hour.

This event can be described as follows:

- **28/02/2018 08:00 - Formation of a convergence zone:** On the 28th of Feb., at 8 am (local time), just before the beginning of the snow storm, temperatures are very cold over lands in the region, in altitude ($-6°$ at 850 hPa, corr. to about 1500 m) and on the ground (between $-2°$ and $6°$ at 2 m). We can observe a line of convergence on the sea, with, on the one side, cold air brought from the northeast related to the cold spell and, on the other side, winds from the southeast bringing warm air. This convergence zone will generate vertical fluxes and will create this atmospheric disturbance at the origin of important snow and rain accumulations.

- **28/02/2021 14:00 - Beginning of the snowfall:** At 2 pm (local time), important precipitation amounts occur around the convergence zone, mainly along the coast but also offshore. At the northwest of this zone (Montpellier, Béziers), despite a slight and progressive increase of temperature at the ground and in altitude, the supply of cold air from the North leads to solid precipitation only.

- **28/02/2018 20:00 - Snow/rain event:** Between 8 pm and 2 am (local time), winds from South-East intensify, and pre-cipitation amounts on Montpellier increase. AROME model shows a temporary movement of the convergence zone from the plains. Then, a northeast flux with cold air at low altitudes leads to snow again in the surroundings of Montpellier.

- **01/03/2018 02:00 - Warming and rainfall gets stronger:** During the night between $28/02/2018$ and $01/03/2018$, warming is rising at high altitudes (from $-3°$ at 6 pm to $0°$ at 2 am at 1500 m) and rainfall becomes dominant.

- **01/03/2018 08:00 Intense rain event:** In the morning of $01/03/2018$, despite the persistence of the convergence zone and cold ground temperatures, warming in altitude is too important and precipitation only falls as rain. The collapse took place at around 18:00.
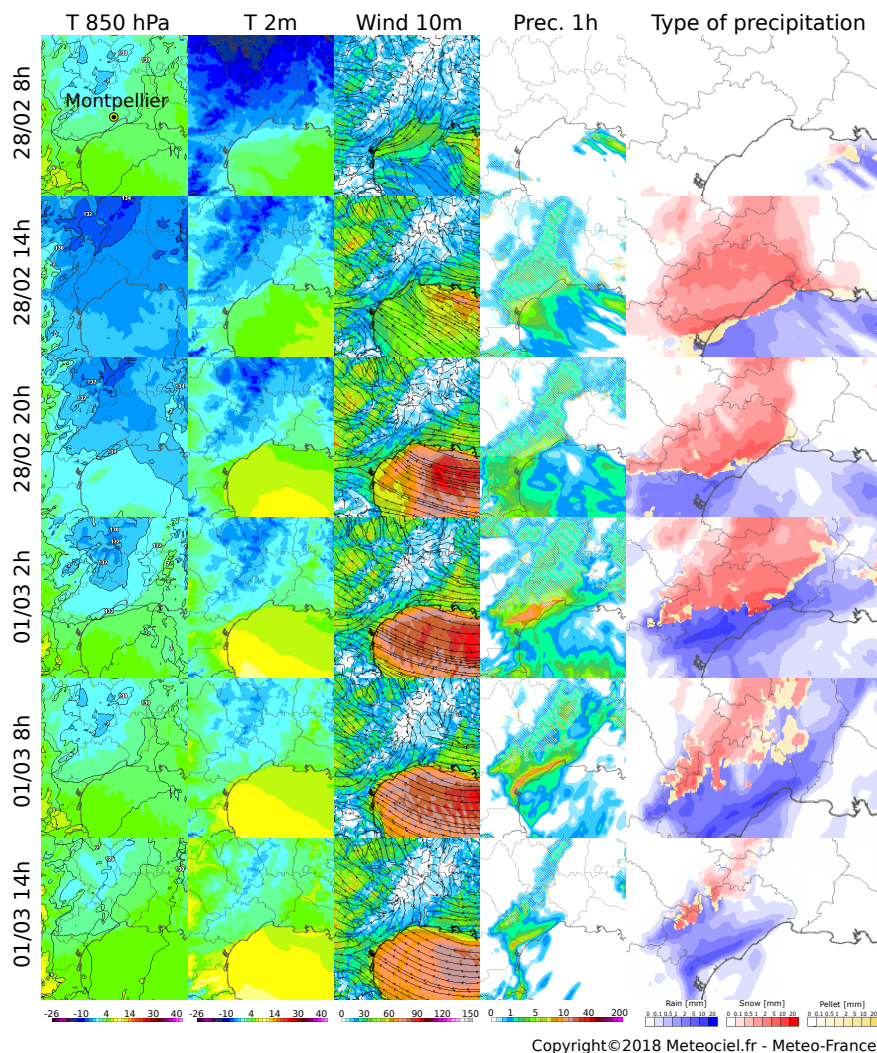
Figure 3. Outputs of the high-resolution AROME model for the following parameters: temperature at 850 hPa [°C], temperature at 2 m [°C], wind at 10 m [km/h], precipitation amount accumulated in 1 hour [mm] and the corresponding type of precipitation (rain, snow or ice pellet). The maps shown on each line correspond to different runs for 1h lead time, from 28/02 at 8:00 to 01/03 at 14:00 (local time). Source: Meteo-France.

2.2 An intense rain-on-snow event

This rain-on-snow event is atypical in the region of Montpellier considering the accumulated amount of precipitation and the amount of precipitation fallen as snow. Ground measurements indicate that snow depths of more than 25 cm have occurred only five times since the 1950s (35 cm in February 1954, 35 cm during the winter 1962-1963, 27 cm on the 14-16/01/1987, 28 cm on the 22/01/1992 and the event described here). The empirical return period of the snow event alone exceeds 10 years

(five events in 70 years). What makes the rain-on-snow event particularly unusual is the large amount of rainfall that followed the snow event. Its occurrence can be explained by the main following elements:

- the presence of very cold air at all altitudes and in particular at the low troposphere;

- the blocking of a strong convergence zone leading to an intense rain/snow event;

- the preservation of this convergence zone and cold wind supply from the northeast around Montpellier.

The last column of Figure 3 presents the evolution of the type of precipitation simulated by the AROME model for 1h lead time. AROME clearly simulates an intense snow event from 28/02/2018 at 14:00 until the end of this day, followed by a rain/snow event during the night. An intense rain event brought large amounts of liquid precipitation during the whole day of 01/03/2018.

2.3 Snow accumulation

Meteo-Languedoc is an association providing various information about weather forecasts and natural risks in the region around Montpellier. This exceptional data is described in detail on their website[1] and includes various information about the meteorological event, including photos from amateurs following their Facebook page[2]. Through their Facebook page, MeteoLanguedoc asked their 120 000 followers to provide observations, and photos supporting these observations. Thanks to the collection of 5 000 feedbacks, a robust estimation of the depth of the snowpack at the end of the snow event was obtained, leading to the interpolated field of snow accumulation provided in Figure 4. The data clearly shows that the snow depth was more important in the North of Montpellier, likely due to a hill separating the city center from the Lavalette site.

2.4 Estimation of the snow load at the time of the collapse

Figure 5 shows the evolution of the temperature, rain, and snow amounts according to two different and independent sources of information:

- Just next to the center of Irstea in Montpellier, a weather station (the Lavalette station) records various meteorological parameters, including temperature and rain. For this station, the tipping-bucket rain gauge is not heated and snow was probably blocking the rain gauge according to the operator of the station.

- SAFRAN reanalysis (Vidal et al., 2010) provides weather parameters at a resolution of 8 km over France, using a dense gauge network. However, this network does not include the station at Lavalette.

Both sources of information clearly show the increase in temperature from the morning of 28/02/2018 until the building collapse. SAFRAN reanalysis records an accumulation of snow water equivalent of 35 mm followed by 58 mm of rainfall

---

[1]https://www.meteolanguedoc.com/evenements-majeurs-en-languedoc-roussillon/episode-neigeux-du-28-fevrier-2018-jusqu-a-35-cm-pres-de-montpellier/p513, last access: 05 September 2023

[2]https://fr-fr.facebook.com/MeteoLanguedoc/, last access: 05 September 2023
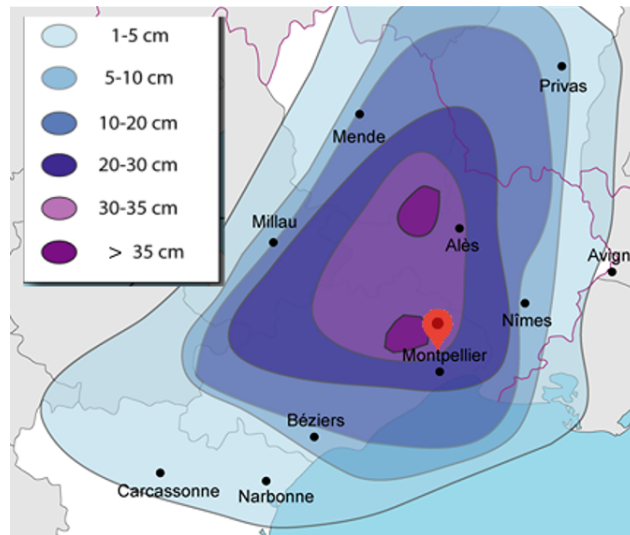
Figure 4. Snow accumulation during the snow event of 28/02/2018, based on 5000 testimonies. The red marker shows the position of the collapsed building. Source: Meteo-Languedoc.

before the collapse, with a rain/snow transition during the night between 28/02 and 01/03. The rain gauge, which might have underestimated the rainfall accumulation due to the presence of snow in the receptacle, records 45 mm.

135 The different sources of information (outputs from AROME model, social network testimonies, weather data) on the snow-and-rain event lead to the following scenario. It can be considered with little uncertainty that the snow depth in the area was between 30 cm and 35 cm, on cold ground. Since the Irstea building was located right next to the 30 cm curve (see Figure 4), 30 cm is considered the best estimate, but there is uncertainty around this estimate.

 The snow had a density of about 250 kg.m^{-3} before the rain event, based on the fact that most of the Facebook testimonies

140 reported a heavy snow type, which is typical of a Mediterranean area. As indicated above, the snowfall has been followed by 50 to 60 mm of rainfall. Colbeck (1977) indicates that rain can contribute up to 50% of the roof load for flat roofs with 10 m parallel flow to gutters, which corresponds closely to the specifications of the Irstea Cévennes building. Figure S5 in the SM shows the roof drainage system of the Irstea Cévennes building. The roof had a slight slope of 1 % on each side of a peak line oriented north-south, which allows rainwater to flow towards the east or west of the building and drain through 20 cm high

145 outlets located at the base of the low walls on the roof edges. There were four outlets at the ends of the northern and southern edges, one in the middle of the western edge, and two at the quarter and three-quarter points of the eastern edge, as indicated by the red arrows in Figure 6a. In our case, it is likely that this drainage system was inefficient due to the combination of both (i) a small roof slope and (ii) large distances between the outlets (13 m in the north-south direction and 40 m in the east-west direction). Colbeck (1977) indicates that "Snow covered roof [...] would certainly collapse if a rainstorm were of sufficient

150 duration to allow complete wetting of the unsaturated layer and full development of the saturated layer". Here, 18 hours of continuous rainfall with an average intensity of around 3 mm/h certainly contributed to the saturation of the snow layer. As
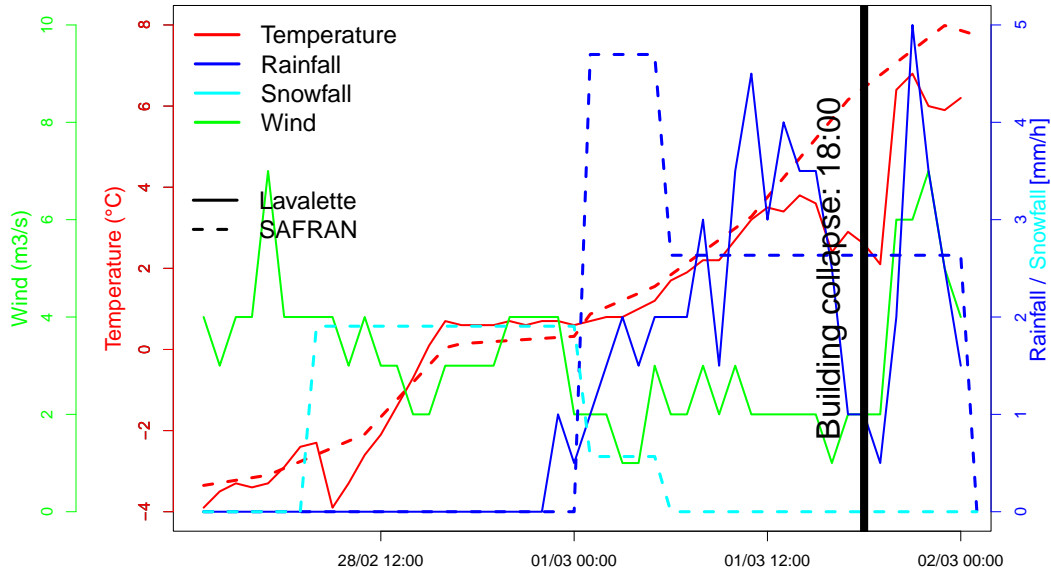
Figure 5. Weather observations at the station of Lavalette (plain lines) and SAFRAN reanalysis at the grid point covering Irstea building (dotted lines).

we are not able to assess the quantity of water that could reach the outlets at the time of the collapse (which also depends on the structure deformation due to the snow load, as discussed below), it is assumed in the present analysis that the total load corresponds to the addition of the snow load and the rain load. We also assume that the initial snow load (before the rain) on the roof is assumed to be equal to the snow load on the ground for several reasons. Firstly, the roof slope was low and there was a small wall around the edges of the roof. Secondly, the wind was not significant enough to modify the snow distribution on the roof. Finally, the observed temperatures suggest that there was no snowmelt during the snowfall event.

In the remainder of this study, we thus assume that at the time of the collapse which occurred on March 1 at around 18:00, the snow-and-rain load is the outcome of 30 cm of initial snow with a density of 250 kg.m^{-3} (which corresponds to a load of about 736 N.m^{-2}) and 50 to 60 mm of rainfall (*i.e.* an additional load of $490 - 589$ N.m^{-2}). This results in a snow-and-rain load of about $1\,226$ to $1\,325$ N.m^{-2}.

3 Modeling of mechanical behavior of the loaded building

3.1 Initial state of the building (before collapse)

The Cévennes building was an experimental hall built in 1982 on the Lavalette domain in Montpellier, in the South East of France. At the time of its failure, it housed a wind tunnel and a mezzanine level built in 2014 along the northern facade, and offices on two floors along the southern facade. Figure 6 gives an overview of the Cévennes building before and after the
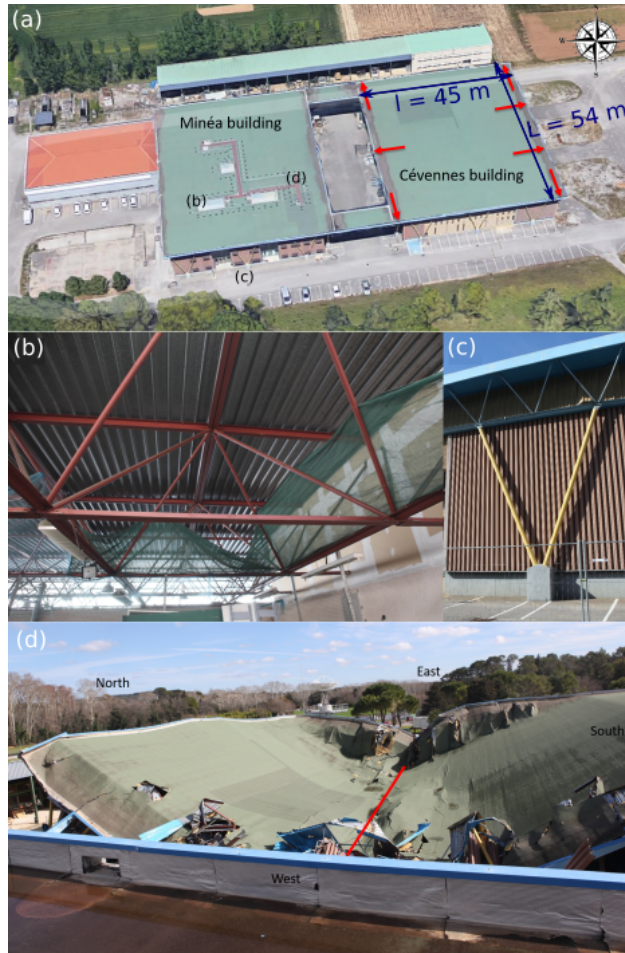
Figure 6. (a) Overview of the Irstea Cévennes building before the damage, with rainwater drainage points indicated by red arrows. The dimensions of the roof are given in blue, and the height of the building is 10 m. The letters indicate where the photos of the other subplots were taken (photo credit: ©Google Earth 2014, adapted by I. Ousset). (b-c) View of the supporting structure of the Irstea Cévennes building before its damage: (b) red-coloured metal roof frame and (c) supporting tubular pylons (in yellow) along the facades. (d) Overview of the damaged Irstea Cévennes building. The red line indicates the direction perpendicular to the direction of the main deflection of the roof after the collapse.

damage. The dimensions of the roof were $l = 45$ m in the east-west direction and $L = 54$ m in the north-south direction and 10 m high.

The supporting structure of the building consisted of three-dimensional vertical metal trusses designed to support the flat roof (see sketches in Figure S1 in the SM), which in turn were supported by metal tubular pylons that were arranged along the facades of the building. The lattice structure, consisting of welded or bolted elements, extends over the entire roof area and resists all forces acting on it. For the southern, western, and northern facades of the building, the tubular pylons consisted

of two round tubular profiles arranged in a V-shape and sealed on concrete blocks anchored to the ground (see photograph in Figure 6c, sketches in Figures S1a,b in the SM and the geometric properties of the structure in Table S1 in the SM). For the east facade of the building, they consisted of rectangular tubular profiles and a Saint Andrew's cross obtained with T-profiles (Figure S1c in the SM). It should be noted that no such tubular pylons were placed inside the building in order to allow the movement of large vehicles, such as agricultural tractors.

The initial state of the building before the event is known with some uncertainty. In particular, past damage may have already occurred before the 2018 event and altered the initial integrity of the structure. For example, although the building studied is not located in an area with intense snow events, it has had to support heavy loads on (at least) three occasions since its construction:

- around 27 cm on January 14-16, 1987;

- around 28 cm on January 22, 1992;

- less than 10 cm on March 7, 2010.

It is important to note that the snow event of January 22, 1992 was probably followed by rain, for which SAFRAN records provide a cumulative amount of 8 mm of rain approximately 36 hours after the snowfall. To the best of our knowledge, no survey of the structure of the Cévennes and Minéa buildings was carried out between the date of their construction and the 2018 incident. Following this event, only a technical opinion on the strength of the adjacent Minéa building was requested. This report concluded that the overall strength of the structure was satisfactory, but identified a number of points requiring vigilance:

- significant stagnation of rainwater on the roof;

- slight buckling (within manufacturing tolerance) and traces of corrosion on some profiles (angles and tubular profiles) at the level of the roof metal frame;

- buckling of one of the profiles of a Saint-Andrew's cross;

- V-columns in satisfactory condition, with slight corrosion on the head and anchor plate;

- presence of cracks (on several blocks) and spalling revealing the reinforcement (on one block) on the basal concrete blocks for anchoring the V-columns.

Given the limited information available on previous events and any damage that may have resulted from temporary loads applied to the structure in the past, this study has not taken into account any such deterioration of the structure.

Finally, it should be noted that no changes were made to the supporting structure from the time of its construction to the time of its collapse. The only changes made were to the interior (ground-supported mezzanines) in 2014.

3.2 Distribution of the snow-and-rain loads on the roof

We have little information about the depth and spatial distribution of the initial snow on the roof. As the entire site was evacuated in the early afternoon of March 1, only the caretaker was present at the time of the building collapse, but he did not observe how the snow was distributed on the roof. Given that the wind velocity on both days was only between 1 and 4 m.s^{-1}, it is unlikely that the wind could have affected the distribution of snow on the roof. However, the distribution of the snow-and-rain load may have varied over time due to a complex interaction between the overall structure and the dynamics of the snow cover, which gradually became wet. It seems likely that the distribution of the initial snow load (before rainfall) was nearly uniform due to the low slope of the roof combined with the light wind during the snowfall. As indicated in Section 2.4, it is assumed that the rainwater remained on the roof until the complete collapse of the building. In order to try to gain some insight into different scenarios of spatial load distribution, three different (virtual) cases are studied, as shown in Figure 7a:

(a) **Uniform distribution**: reference case where the load distribution due to snow and rain is uniformly distributed,

(b) **Non-uniform with greater water depth at the edges**: water flowed rapidly towards the edges of the roof (assuming that the slope angle was sufficient),

(c) **Non-uniform with greater water depth in the center**: water mainly accumulated in the center of the roof.

For the two non-uniform distributions, we considered a snow load distribution that was initially uniform before rain came into play, as in the first case.

3.3 FE simulations

In order to investigate in detail the mechanical response of the Irstea Cévennes building and thus better understand its collapse under the snow-and-rain load, the metal supporting structure was modeled using different Abaqus Finite Element (FE) models (see Section S2 in the SM for additional details). Two types of analysis are performed:

1. The **pushover analysis** provide load values associated with different types of failure criteria which can be interpreted as critical impacts on the structure with different levels of severity,

2. The **buckling analysis** indicate what specific elements of the structure were the most likely to be at the origin of the roof collapse.

Pushover analyses are quasi-static analyses (without dynamic effects) that determine how far the building can go before it collapses completely or partially. Figure 7 illustrates the main steps of this analysis. The first step (Step 1 in Figs. 7b-c) takes into account the self-weight of the structure. Then the snow-and-rain pressure on the structure is gradually and linearly incremented to mimic the load increase during the rain-on-snow event until the structure fails by reaching either the elastic limit of the material or the ultimate limit of the material for a snow-and-rain pressure equal to the failure force. This linear increase is performed in one step for uniform loads (step 2 in Fig. 7b) and two steps for non-uniform loads (steps 2 and 3

in Fig. 7c). In the latter case, step 2 corresponds to the increase of the uniform load of snow before the rain whereas step 3 corresponds to the increase of the non-uniform load of water on the snowpack.
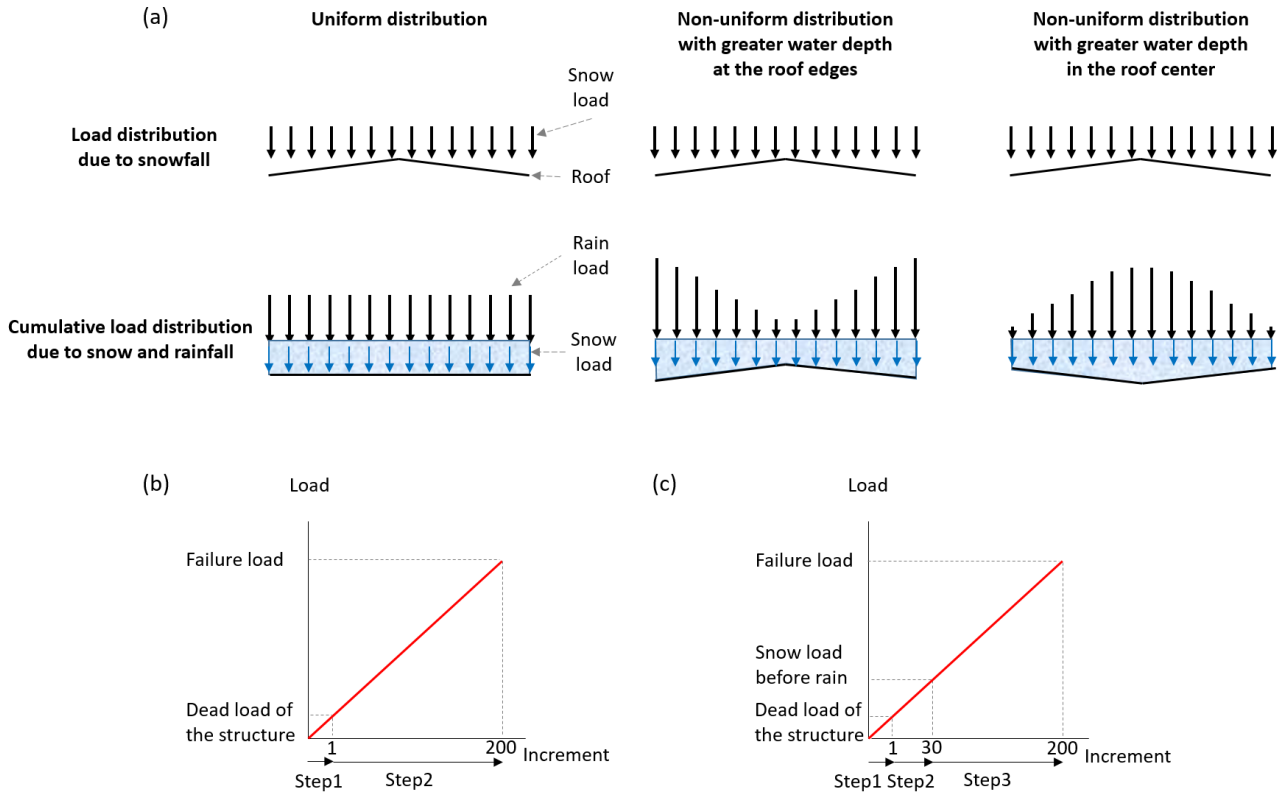
Figure 7. (a) Different assumptions made for the spatial distribution of snow-and-rain loads and (b), (c) load evolution by incrementation for pushover analyses in the cases of a uniform distribution (b) and a non-uniform distribution (c) of rain loads. Note that the increment numbers of steps 2 and 3 are given here as examples only.

Secondly, a non-linear buckling analysis is carried out in two steps:

1. A linear or eigenvalue buckling analysis is performed to obtain the theoretical load values at which buckling of the structure, idealized as elastic, occurs with different buckling mode shapes (so-called eigenvalue modes), as shown in Figure 8. This analysis is carried out by using the subspace iteration method (a simple method for approximating the eigenvalues of matrices), after a static step that takes into account the self-weight of the structure;

2. A non-linear buckling analysis is performed by using the incremental static Riks procedure of Abaqus, integrating material non-linearities and geometric imperfections corresponding to the displacement results of the linear buckling analysis, in order to estimate the most realistic critical buckling bifurcation pressure. Only the first mode shape is considered to define the geometric imperfections. The corresponding displacements are multiplied by an argument equal to 1% of the

thickness of the crossbar, *i.e.* 0.5 mm, which corresponds to the manufacturing tolerance of a round tubular profile with an external diameter of less than 75 mm.

These numerical tests do not describe the full (dynamic) collapse of the roof, but are intended to identify the critical loads at which significant deformation and damage could start to occur before the collapse, considering different failure criteria (FC):

- FC_{BD}: deflection threshold equal to 0.225 m, which corresponds to the acceptable beam deflection (vertical displacement that can be observed at the center of the roof) equal to 1/200 of the width of the building $l = 45$ m;

- FC_{HD}: horizontal displacement threshold at the top of the columns equal to $H/150 = 0.047$ m;

- FC_y: critical stress state with an accumulation of stresses equal to the yield strength of steel in a given location of the FE model. This so-called *elastic limit* indicates the limit of the elastic behavior of the structure, i.e. the beginning of irreversible deformations;

- FC_u: critical stress state with an accumulation of stresses equal to the ultimate strength of steel. This so-called *ultimate limit* of the material corresponds to the maximum load that the structure can withstand before a local material rupture;

- FC_{LB}: first eigenvalue buckling load assessed by the linear buckling analysis;

- FC_{NLB}: non-linear buckling load corresponding to the bifurcation buckling load that causes the actual buckling, taking into account the geometric imperfections.

The first two failure criteria deal with global damage to the structure and are part of the Serviceability Limit States (SLS). The other failure criteria correspond to Ultimate Limit States (ULS). These criteria indicate the onset of deterioration that could potentially have a significant impact on the structure and ultimately lead to its collapse.

Table 1 summarizes the different critical load values obtained from the FE simulations that lead to the failure of the structure, considering the different criteria mentioned above, under the three different assumptions of snow-and-rain load distribution. The values obtained for these critical loads vary over a wide range from 645 to 3410 N.m^{-2} depending on the failure criterion and the distribution of the pressure field. Section 4 further discusses these different critical loads and compares them with the estimated snow-and-rain load of about 1226 to 1325 N.m^{-2} provided in Section 2.

The FE simulations allow us to gain further insight into the detailed behavior of the structure. Figure 9 shows the stress fields of the structure obtained from the pushover simulations and corresponding to the three types of distribution for a snow-and-rain load of 1325 N.m^{-2}. In the three cases, the maximum stresses occur on the crossbars located at the perimeter of the roof (above the western and eastern facades in the two first cases and above the four facades in the last case) and, in the cases of uniform distribution and non-uniform distribution with greater water depth in the center, on the bottom horizontal T-profiles located in the central part of the roof. Stresses (slightly) above the yield strength of the material occur only on two crossbars located above the east facades and are prone to buckling.

The results of the linear buckling analysis for a uniform snow-and-rain pressure field are summarized in Table 2 and in Figure 8. The analysis shows that buckling occurs locally. For each of the eight first eigenvalue modes considered, only one or

Table 1. Load values leading to the failure of the supporting structure calculated from the FE simulations according to different failure criteria (see text for details), and considering three scenarios for the distribution of the snow-and-rain load: uniform distribution (snow and rain), non-uniform distribution with greater water depth at the edges after uniform snowfall, and non-uniform distribution with greater water depth in the center after uniform snowfall. The last line of the table indicates the loads at which code divergence was observed (when the considered failure criterion was not reached).

	Failure criterion	Notation	Load value [N.m^{-2}]		
			Snow-and-rain distribution:		
			Uniform	Greater water depth	
				at the edges	in the center
SLS	Deflection threshold	FC$_{BD}$	1 360	1 660	1 205
	Horizontal displacement threshold	FC$_{HD}$	2 350	Not reached	1 915
ULS	Elastic limit	FC$_y$	1 330	1 345	1 325
	Ultimate material limit	FC$_u$	3 410	Not reached	Not reached
	Linear buckling	FC$_{LB}$	935	930	940
	non-linear buckling	FC$_{NLB}$	645	645	645
	Code divergence		-	2 700	2 010

two crossbar(s) located at the western or eastern perimeter of the roof and on either side of the east-west axis of the structure buckle with a shape similar to that of the first and fifth modes shown in Figure 8. Table 2 provides information on the buckling load, displacement, and location of crossbars prone to buckling for each eigenvalue mode. It shows that buckling occurs first at the crossbars above the western facade and then above the eastern facade. Similar results (not shown) are obtained for the other two cases of non-uniform snow-and-rain pressure distribution with greater water depth either at the edges or in the center of the roof.

These results clearly indicate that the failure was due to both buckling of the crossbars (primary cause) and bending of the bottom horizontal T-profiles (aggravating effect). Other damage, such as that observed on the round tubular columns shown in Figure S3c-d in the SM, probably occurred during the collapse of the structure. No such damage was observed on the nearby building, whereas slight buckling was observed on its roof. This subsequent damage was further modified by the presence of the offices and mezzanine walls along the northern and southern facades (see Fig. S3e in the SM).

4 Discussion

This section aims to further link the results from the snow-and-rain hazard (Section 2) and from the FE simulations that include pushover tests and a buckling anlysis (Section 3) to identify the most probable factors that led to the collapse of the Irstea Cévennes building.

Table 2. Results of the eigenvalue buckling analysis of the structure (linear buckling) under a uniform snow-and-rain pressure field.

Eigenvalue mode	Corresponding load [N.m^{-2}]	Corresponding displacement [m]	Location of the buckling crossbars
1	934.6	1.373	Western facade
2	937	1.366	Western facade
3	939	1.279	Western facade
4	941.1	1.277	Western facade
5	1051.3	1.241	Eastern facade
6	1055.5	1.392	Eastern facade
7	1099.6	1.318	Eastern facade
8	1105.2	1.353	Eastern facade
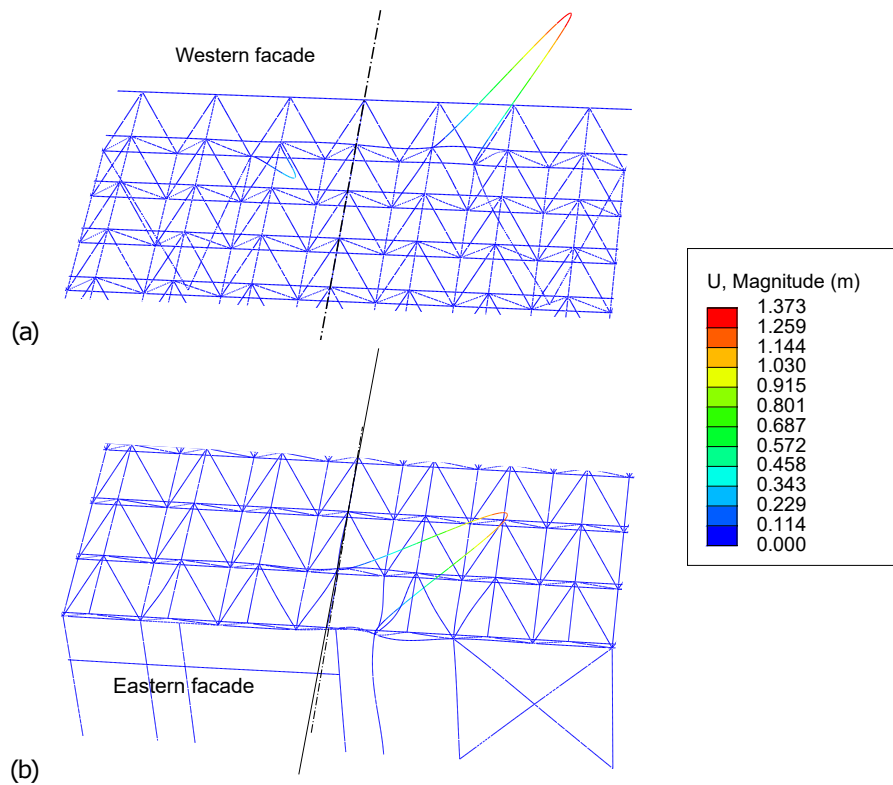
Figure 8. Buckling mode shapes of the structure under a uniform snow-and-rain pressure field (deformation scale factor = 5.4): (a) first mode, above the western facade and (b) fifth mode, above the eastern facade.

4.1 Building collapse analysis under the rain-on-snow event of February 2018

Figure 10 compares the critical loads that would cause a failure according to the FE simulations (Table 1) with the initial snow load of 736 N.m^{-2} before the rain and the final snow-and-rain load values of $1\,226$ to $1\,325$ N.m^{-2} estimated from different source of observations in Section 2.

The maximum critical load of $3\,410$ N.m^{-2} (in red in Figure 10) corresponds to the ultimate limit of the material under uniform pressure distribution and is well above the estimated value for the snow-and-rain load of $1\,226 - 1\,325$ N.m^{-2} (in cyan). Note that for non-uniform snow pressure fields, the ultimate material limit is not reached due to numerical instabilities (lack of convergence). The values obtained from the horizontal displacement criterion are also quite above the estimated range of $1\,226 - 1\,325$ N.m^{-2}. The pushover FE simulations thus suggest that neither the ultimate material limit nor the critical horizontal displacement was reached at the time just before of the collapse, regardless of the scenario for rain load spatial distribution.

The minimum of 645 N.m^{-2} (in brown) corresponds to the non-linear buckling load. This value is just below the uniform initial snow load before the rain (736 N.m^{-2}) (in teal) and does not depend on the assumption made for the distribution of the rain load. In contrast, the linear buckling analysis gives higher values for the load corresponding to the first eigenvalue mode (from 935 to 945 N.m^{-2}). All of these critical buckling loads (in beige) are well below the snow-and-rain load estimates. This means that this failure can have occurred with the observed snow-and-rain load. In addition, although it should be noted that the buckling failures remained localized (on a few crossbars located at the eastern and western edges, as shown in Section 3 and Figure 8), they occur on both sides of the east-west axis along which the structure collapsed, as shown in Figure 6d. Thus, it is very likely that buckling was involved at some stage in the roof collapse.

For a uniform load distribution, the other failure criteria (the elastic limit and the beam deflection) give intermediate values in the range $1\,330 - 1\,360$ N.m^{-2}, just above the snow-and-rain load estimates. For the scenario with greater water depth at the edges, the critical load values increase, particularly for the beam deflection criterion, which puts the structure on the safe side. For the scenario with water flowing towards the center of the roof, both critical load values (elastic limit, beam deflection) decrease close to or below the snow-and-rain load estimates.

In summary, the FE simulations indicate different situations where the critical load values were below (or very close to) the snow-and-rain load estimates and thus could lead to critical damage and failure of the structure during the 2018 snow-and-rain event. According to the linear and non-linear buckling analysis, buckling has likely been critical regardless of the scenario for the distribution of the snow-and-rain load, indicating a weakness in the structure. In addition, based on the elastic limit criterion and the beam deflection criterion, load concentration in the center of the roof (most likely due to water accumulation in the center of the roof) has probably been at some stage an aggravating factor. However, it must be pointed out that the order and the interactions between these different mechanical responses (buckling, beam deflection) are not taken into account by the FE simulations.

4.2   Structural back analysis

In Section S3 of the SM, we discuss in detail the regulations on snow action on structures: those in force at the time of the construction of the Irstea Cevennes building and those in force at the time of the building collapse. By comparing the regulations with the FE-Abaqus calculations in terms of the load applied to the structure, we show that the Irstea Cevennes building was certainly built correctly according to the previous French regulations (of 1965), if we do not take into account the results of the non-linear buckling analysis, since the consideration of imperfections in the design of metal structures was introduced in the regulations after the construction of this building (in 1983). It can also be concluded that, at the time of its collapse in 2018, the building did not comply with the new regulations; in fact, the critical buckling load of the structure (estimated at 645 N. m^{-2}) was lower than the design accidental snow load resulting from the Eurocode (equal to $1\,280$ N.m^{-2}, see Section S3 in the SM).

This subsection aims to identify the weaknesses of the structure subjected to the extreme climatic event (the estimated snow-and-rain load of $1\,226 - 1\,325$ N.m^{-2} was indeed close to the design exceptional snow load specified in the Eurocode, see Figure S8 of the SM) to possibly explain the collapse. Firstly, as indicated above, the crossbars at the eastern and western perimeter of the lattice roof were clearly prone to buckling. Although this buckling was localized, it gradually weakened the structure and could have potentially contributed to its collapse. Similar phenomena were also observed in the nearby building after the 2018 incident (Fig. 6). Secondly, since large vehicles (agricultural tractors) were to be used inside the building, no load-bearing walls were built inside. This resulted in a very large span of the roof supporting lattice. Even if the deflection threshold FC_{BD} is respected, the FE simulations show that the snow-and-rain has led to an important deflection of the lattice (Fig. 9). It should be noted that the nearby building, similar to the one that collapsed, resisted the February 2018 event and is still standing on the site. This nearby building contains a number of offices and therefore has some internal load-bearing walls. This may be an indication that these latter walls within the structure are likely to be effective in preventing significant deflection.

Finally, the roof rain drainage system, consisting exclusively of vertical openings located in the lower part of the roof perimeter (see Figure S5 in the SM) combined with a near-flat roof, probably contributed to a very poor evacuation of the rain immediately after the snow event, leading to a significant increase in the load carried by the roof. In the future, it would be interesting to perform more thorough studies of rainwater drainage on near-flat roofs during rain-on-snow events, following the efforts made by Colbeck (1977); O'Rourke and Downey (2001); Otsuki et al. (2017). It is important to clarify the effectiveness of different drainage solutions under snowy roof conditions, and to make appropriate recommendations regarding the required roof slopes and the selection and design of downstream drainage devices.

5   Conclusions

Using multiple sources of information regarding the 2018 meteorological event in terms of snow and rain amounts and detailed simulations of the behavior of the roof structure subject to loads, this study provides a detailed back analysis of the interactions between the snow cover and the structure. Concerning the meteorological event, while intense snow events are unusual in this area, this type of event can occur when winter storms bring important masses of cold air from northern Europe to the south (see

the recent event in Madrid Smart, 2021). In Montpellier, snow depths around or above 30 cm have been recorded several times in the past (35 cm in February 1954, 35 cm during winter 1962-1963, 27 cm on the 14-16th of January 1987, 28 cm on the 22nd of January 1992). For this event in Montpellier, the snow-rain transition led to a saturated and overweight load. A detailed understanding of the meteorological event has been consolidated using various sources of information: weather stations, numerical weather model outputs, meteorological reanalysis, and numerous testimonies obtained using social networks (Facebook).

This study proposes an assessment of the response of the structure to incremented load values under quasi-static conditions, as well as a buckling analysis. Different scenarios for the distribution of the pressure field imparted to the structure have been studied. Based on the results obtained, the collapse of the Irstea Cévennes building can be explained by a combination of several factors. First, the structure was susceptible to significant buckling and, to a lesser extent, to bending (although it was designed in accordance with the regulations on this aspect). Secondly, the collapse was probably caused by the rain-on-snow surcharge. Furthermore, it seems evident that geometric imperfections were not considered in the design of the structure, resulting in its vulnerability to buckling (also observed in the neighbouring Minea building). The fact that the resulting load exceeded the critical load leading to roof failure is certainly due to the additional water on the initial snowpack. Such a rain-on-snow scenario is considered in the regulations but it appears that in the particular chronicle of the 2018 event (significant amounts of snow and then rain), the resulting overload was greater than the design scenario.

Code/Data availability

SAFRAN meteorological data are owned by Météo-France and are not freely available. Meteorological data from the Lavalette station and the codes/data used to implement Abaqus Finite Element models are available upon reasonable requests by directly contacting the corresponding author.

Author contributions

TF coordinated and supervised the back-analysis study. GE and DR performed the meteorological event analysis. IO carried out the FE model simulations. All authors discussed the results and co-wrote the manuscript.

Competing interests

The authors declare that they have no conflict of interest.

Acknowledgments

The authors thank Mohamed Naaim for having motivated this research. They are grateful to Meteo-Languedoc and Meteociel for sharing the meteorological information and resources. They also thank Jean-Luc Descrismes and Sylvain Labbé of INRAE

for having provided all available information about the Irstea Cévennes building. Finally, the authors are grateful to the Editor, Yves Bühler, and to the numerous referees for their insightful comments on previous versions of the manuscript.

References

385 AFNOR: NF EN 1991-1-3/NA : Eurocode 1 : Actions sur les structures - Partie 1-3 : Actions générales - charges de neige. Annexe nationale
à la NF EN 1991-1-3, Association Francaise de Normalisation (AFNOR), 2007.

Altunişik, A., Ateş, S., and Hüsem, M.: Lateral buckling failure of steel cantilever roof of a tribune due to snow loads, Engineering Failure
Analysis, 72, 67–78, https://doi.org/10.1016/j.engfailanal.2016.12.010, 2017.

ASCE: Minimum Design Loads for Buildings and Other Structures - ASCE/SEI 7-10, Tech. rep., https://law.resource.org/pub/us/cfr/ibr/003/
390 asce.7.2002.pdf, 2013.

Biegus, A. and Kowal, A.: Collapse of halls made from cold-formed steel sheets, Engineering Failure Analysis, 31, 189–194,
https://doi.org/10.1016/j.engfailanal.2012.12.009, 2013.

Biegus, A. and Rykaluk, K.: Collapse of Katowice Fair Building, Engineering Failure Analysis, 16, 1643–1654,
https://doi.org/10.1016/j.engfailanal.2008.11.008, 2009.

395 Bouttier, F. and Roulet, B.: Arome, the new high resolution model of Meteo-France, The European forecaster - Newsletter of the WGCEF
(Printed by Meteo-France), 13, 27–30, 2008.

Brencich, A.: Collapse of an industrial steel shed: A case study for basic errors in computational structural engineering and control proce-
dures, Engineering Failure Analysis, 17, 213–225, https://doi.org/10.1016/j.engfailanal.2009.06.015, 2010.

Caglayan, O. and Yuksel, E.: Experimental and finite element investigations on the collapse of a Mero space truss roof structure – A case
400 study, Engineering Failure Analysis, 15, 458–470, https://doi.org/10.1016/j.engfailanal.2007.05.005, 2008.

Canadian Commission on Building and Fire Codes: National Building Code of Canada: 2010, Tech. rep., National Research Council of
Canada, https://doi.org/10.4224/40001268, 2010.

Colbeck, S. C.: Roof loads resulting from rain on snow: results of a physical model, Canadian Journal of Civil Engineering, 4, 482–490,
https://doi.org/10.1139/l77-057, 1977.

405 del Coz Díaz, J., Álvarez Rabanal, F., García Nieto, P., Roces-García, J., and Alonso-Estébanez, A.: Nonlinear buckling and fail-
ure analysis of a self-weighted metallic roof with and without skylights by FEM, Engineering Failure Analysis, 26, 65–80,
https://doi.org/10.1016/j.engfailanal.2012.07.019, 2012.

Geis, J., Strobel, K., and Liel, A.: Snow-Induced Building Failures, Journal of Performance of Constructed Facilities, 26, 377–388,
https://doi.org/10.1061/(ASCE)CF.1943-5509.0000222, 2012.

410 Geis, J. M.: The Effects of Snow Loading on Lightweight Metal Buildings with Open-Web Steel Joists, Master's thesis, University of
Colorado, http://localhost/files/n583xv25x, 2011.

Holický, M. and Sýkora, M.: Failures of Roofs under Snow Load: Causes and Reliability Analysis, American Society of Civil Engineers, pp.
444–453, https://doi.org/10.1061/41082(362)45, 2009.

Krentowski, J., Chyzy, T., Dunaj, P., and Dunaj, P.: Delayed catastrophe of a steel roofing structure of a shopping facility, Engineering Failure
415 Analysis, 98, 72–82, https://doi.org/10.1016/j.engfailanal.2019.01.082, 2019.

Le Roux, E., Evin, G., Eckert, N., Blanchet, J., and Morin, S.: Non-stationary extreme value analysis of ground snow loads in the French
Alps: a comparison with building standards, Natural Hazards and Earth System Sciences, 20, 2961–2977, https://doi.org/10.5194/nhess-
20-2961-2020, 2020.

O'Rourke, M. and Downey, C.: Rain-on-Snow Surcharge for Roof Design, Journal of Structural Engineering, 127, 74–79,
420 https://doi.org/10.1061/(ASCE)0733-9445(2001)127:1(74), publisher: American Society of Civil Engineers, 2001.

O'Rourke, M. and Wikoff, J.: Snow-Related Roof Collapse during the winter of 2010-2011: Implications for Building Codes, American Society of Civil Engineers, https://doi.org/10.1061/9780784478240, 2014.

Otsuki, M., Takahashi, T., Saito, Y., Tsutsumi, T., and Hitomitsu, K.: Study on evaluation of roof snow load considering rain-on-snow surcharge: Statistical evaluation of snow cover and precipitation in winter in Japan, in: Snow engineering: recent advances, pp. 166–172, ICSE 2016, 8th International Conference on Snow Engineering, June 14-17, 2016, Nantes, France, 2016.

Otsuki, M., Takahashi, T., Tomabechi, T., Chiba, T., Tsutsumi, T., Kamiishi, I., Kikitsu, H., Iwata, Y., Ishihara, T., and Okuda, Y.: Study on Estimation Method for Surcharge Snow Load Due to Rainfall, Journal of Structural and Construction Engineering (Transactions of AIJ), 82, 1329–1338, https://doi.org/10.3130/aijs.82.1329, 2017.

Piroglu, F. and Ozakgul, K.: Partial collapses experienced for a steel space truss roof structure induced by ice ponds, Engineering Failure Analysis, 60, 155–165, https://doi.org/10.1016/j.engfailanal.2015.11.039, 2016.

Piskoty, G., Wullschleger, L., Loser, R., Herwig, A., Tuchschmid, M., and Terrasi, G.: Failure analysis of a collapsed flat gymnasium roof, Engineering Failure Analysis, 35, 104–113, https://doi.org/10.1016/j.engfailanal.2012.12.006, special issue on ICEFA V- Part 1, 2013.

Smart, D.: Storm Filomena 8 January 2021, Weather, 76, 98–99, https://doi.org/10.1002/wea.3950, 2021.

Strasser, U.: Snow loads in a changing climate: New risks?, Natural Hazards and Earth System Sciences, 8, https://doi.org/10.5194/nhess-8-1-2008, 2008.

Takahashi, T., Takahiro, C., and Kazuki, N.: Structural damage caused by rain-on-snow load in Japan, in: Snow engineering: recent advances, pp. 173–178, ICSE 2016, 8th International Conference on Snow Engineering, June 14-17, 2016, Nantes, France, 2016.

Vidal, J.-P., Martin, E., Franchistéguy, L., Baillon, M., and Soubeyroux, J.-M.: A 50-year high-resolution atmospheric reanalysis over France with the Safran system, International Journal of Climatology, 30, 1627–1644, https://doi.org/10.1002/joc.2003, 2010.

Winter, S. and Kreuzinger, H.: The Bad Reichenhall ice-arena collapse and the necessary consequences for wide span timber structures, in: 10th World Conference on Timber Engineering, vol. 4, pp. 1978–1985, Miyazaki, Japan, 2008.
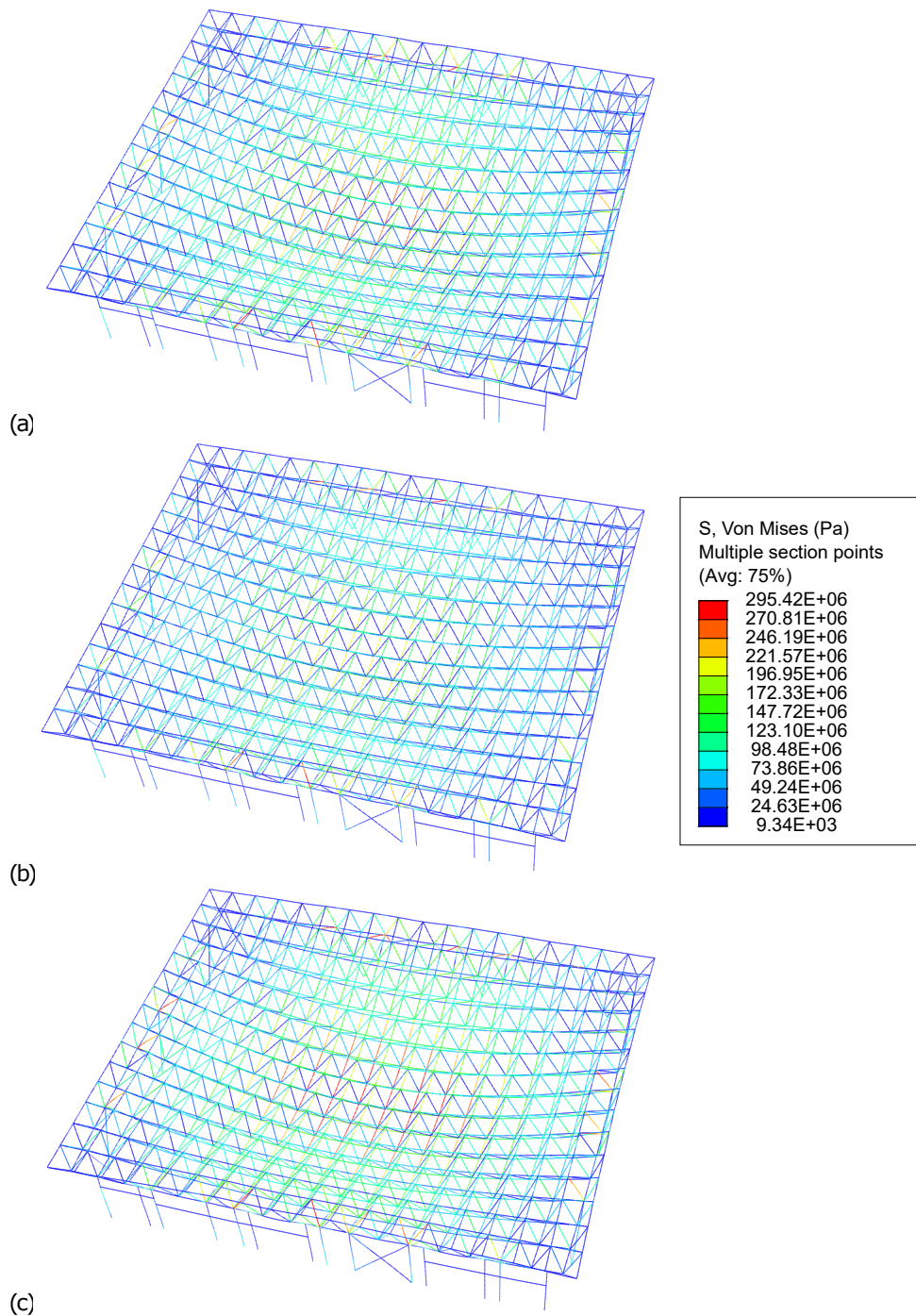
Figure 9. Von Mises stress field (Pa) inside the structure at the real snow-and-rain load of $1\,325$ N.m^{-2}, given by the FE model simulation for the different assumptions made for the spatial distribution of snow and rain: (a) uniform, (b) non-uniform with greater water depth at the edges and (c) non-uniform with greater water depth in the center (a deformation scale factor of 25 is applied to highlight the contrasts).
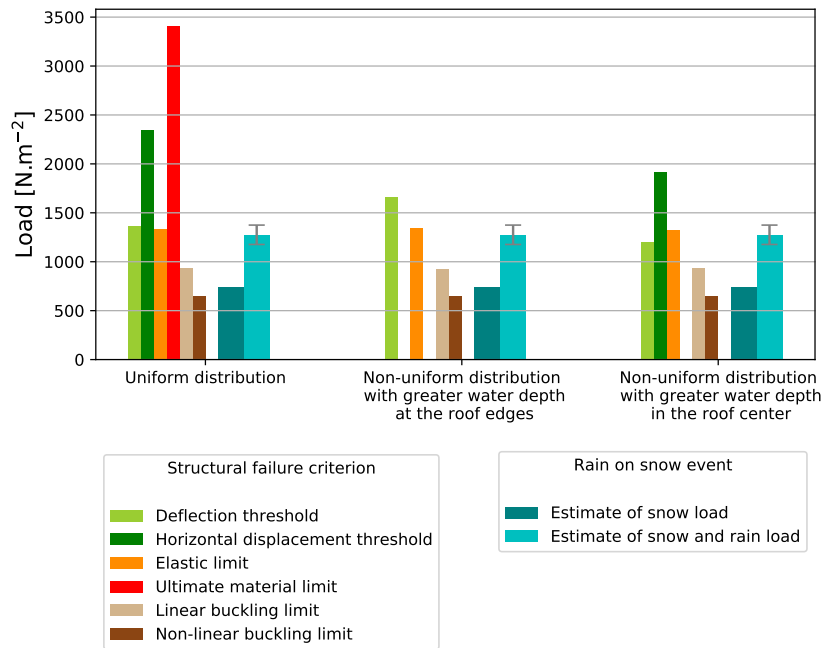
Figure 10. Comparison of the snow loads leading to different failure criteria of the Cévennes building, as calculated by FE model simulations, with the estimated scenario for the rain-on-snow event of 2018, as back-analyzed in Section 2, in the different cases of snow-and-rain pressure field. The structure fails when the observed snow-and-rain load (on the right, for each assumption of snow-and-rain distribution) is greater than a calculated failure load (on the left). The latter calculated failure load could not be obtained when code divergence was observed, thus explaining some empty bars in the case of non-uniform rain distributions (see Table 1).